

# Damage Identification of Bridge Based on Multi-branch Convolutional Neural Network under Moving Load

Chao Wang<sup>1,2\*</sup>, Han Zhang<sup>1</sup>, Gui-Ning Han<sup>1</sup>, Dan Li<sup>3</sup>

<sup>1</sup> Department of Road and Bridge Engineering, School of Civil Engineering, Hubei University of Technology, Nanli Road No. 28, 430068 Wuhan, China

<sup>2</sup> Key Laboratory of Health Intelligent Perception and Ecological Restoration of River and Lake, Ministry of Education, Civil Engineering Building, No. 28, Nanli Road, 430068 Wuhan, China

<sup>3</sup> School of Civil Engineering, Southeast University, Civil Engineering Teaching and Research Building, No. 2, Southeast University Road, Jiangning District, 211189 Nanjin, Jiangshu, China

\* Corresponding author, e-mail: [cwang@hbut.edu.cn](mailto:cwang@hbut.edu.cn)

Received: 23 January 2026, Accepted: 12 April 2026, Published online: 28 April 2026

## Abstract

To address the challenge of detecting damage in a large number of in-service small and medium-span bridges, this study proposes a damage identification method based on a multi-branch convolutional neural network (CNN) under moving loads. Two CNN architectures—a dual-branch model and a multi-branch model—are developed for structural damage identification. The sensitivity of damage identification to sensor location is also investigated. First, various damage scenarios are simulated using a finite element model of a bridge. The structure is excited by a moving vehicle load, and the resulting structural vibration responses are extracted through transient analysis. These responses are then used as input to train and validate the established CNN models. Finally, the effectiveness and accuracy of the proposed method are verified through a laboratory-scale model test. The results demonstrate that both the dual-branch and multi-branch CNN models exhibit higher computational efficiency and better identification performance than a single-branch CNN model under multiple damage scenarios. Furthermore, the identification results show no obvious difference among sensors placed at different locations for the same damage case.

## Keywords

damage identification, convolutional neural network, moving load, finite element analysis, bridge damage

## 1 Introduction

During the long-term service of bridge structures, various factors such as design and construction defects, overloading, environmental corrosion, and material aging can lead to progressive damage and, in severe cases, structural collapse. To monitor operational conditions and assess structural performance, structural health monitoring systems (SHMS) have been installed on many critical long-span bridges [1, 2]. However, due to high implementation costs, the vast majority of small and medium-span simply supported bridges remain unequipped with SHMS. Consequently, the development of rapid and cost-effective damage diagnosis techniques represents a critical and urgent research priority.

Conventional damage identification methods predominantly rely on dynamic testing and can be categorized into model-based and data-driven approaches. Model-based methods diagnose structural damage by comparing changes

in dynamic parameters—such as natural frequencies, mode shapes, modal strain energy, frequency response functions, and flexibility matrices before and after damage occurs [3, 4]. Although these methods are physically well-founded, their accuracy heavily depends on the precision of the finite element model and can be significantly affected by various disturbances. Therefore, their application in real-world engineering remains challenging and requires further investigation.

In contrast, data-driven methods directly analyze structural response data to establish correlations between the response and damage indicators. Techniques in this category include various wavelet transforms [5], Hilbert–Huang transforms [6], and time-series model methods [7]. Most dynamic testing based approaches employ ambient vibrations as excitation, which typically exhibit low signal-to-noise ratios and can thereby degrade damage identification performance.

In response, some researchers have explored damage identification techniques utilizing structural responses under moving loads. For instance, Kong et al. [8] derived the relationship between the response transfer ratio of a vehicle-bridge coupled system and bridge condition parameters, proposing a damage identification method based on this ratio. Nie et al. [9] introduced a moving principal component analysis method for bridge condition monitoring under moving vehicle loads. Similarly, Chen et al. [10] and Zheng et al. [11] developed damage identification techniques based on bridge influence lines extracted from vehicle-induced structural responses. A persistent challenge across these conventional methods, however, is the extraction of damage indicators that are sensitive to structural damage while remaining robust against noise.

In recent years, deep learning techniques have been increasingly applied to structural damage detection [12], as they can automatically extract damage-related features from raw input data. For example, Abdeljaber et al. [13] trained a CNN model using simulated damage data to identify bolt loosening, with training data generated from measured acceleration responses under various simulated damage scenarios. Lin et al. [14] trained a CNN based on a finite element model of a simply supported beam, demonstrating that frequency bands, vibration modes, and their combinations could be effectively learned as key features for damage identification. Yu et al. [15] developed a one-dimensional convolutional neural network (1D-CNN) to localize and quantify structural damage in a five-story benchmark building. However, when damage occurs simultaneously at multiple locations, the classification labels required for a single-branch network increase substantially, often leading to a significant decline in identification accuracy. To address this, Azimi and Pekcan [16] proposed a dual-branch CNN model that processes time-domain data through a 1D-CNN branch and time–frequency-domain data through a 2D-CNN branch, enhancing robustness in damage identification. Li et al. [17] further demonstrated the superiority of multi-label CNNs combined with recurrence plots for diagnosing structural damage under nonstationary excitation. Nevertheless, 2D-CNNs generally demand large datasets and considerable computational resources. Zhang et al. [18] implemented damage detection in T-beam bridges using a deep convolutional neural network, while Xue et al. [19] conducted a three-layer frame model experiment by applying nodal excitation and using structural deflection as input to a 1D-CNN, achieving high identification accuracy. However, for actual bridge structures, responses are typically obtained under ambient excitation with low signal-to-noise ratios, and nodal excitation is often impractical in real-world applications.

In this context, the present study proposes a multi-branch convolutional neural network-based methodology for identifying multi-location and multi-level damage in bridges under moving load excitation. Moving loads provide stronger excitation with higher signal-to-noise ratios and enable faster field testing compared to ambient vibration methods. Two CNN architectures—a dual-branch and a multi-branch model are developed and compared with a conventional single-branch CNN for structural damage identification. The sensitivity of damage identification to the distance between the damage location and the measurement point is also examined. The proposed approach uses a moving inspection vehicle to excite the bridge, and the vertical acceleration response of the structure is recorded. The collected data are then fed into single-branch, dual-branch, and multi-branch CNN models for training and testing. First, finite element analysis is performed to generate various damage samples under multiple damage scenarios. The three CNN models are constructed and iteratively trained and validated. Their identification performances are subsequently compared. Finally, the method is validated through numerical simulations and experimental tests on simply supported beams.

## 2 Damage identification method based on CNN

### 2.1 Convolutional neural network(CNN)

CNN is a supervised multi-layer feed-forward deep neural network capable of automatically extracting damage-sensitive features through supervised training to distinguish various structural conditions. A typical deep CNN architecture comprises input, convolution, pooling, dropout, fully connected, and output layers. The input layer receives the raw test data. The convolution layer, as the core component of a CNN model, extracts local features by convolving the previous layer's output with a set of learnable kernels; the resulting feature maps then serve as input to the subsequent layer. Smaller-sized convolution kernels are employed to capture detailed characteristic of the signal, whereas larger-sized kernels are used to extract global features. The specific operation is described as follow:

$$\mathbf{P}_y^l = f_l \left( \sum_{i=1}^N \mathbf{P}_y^{l-1} * \mathbf{K}_{iy}^l + \mathbf{b}_y^l \right), \quad (1)$$

where  $\mathbf{P}_y^l$  is the  $y^{\text{th}}$  element in the  $l^{\text{th}}$  layer, and  $\mathbf{P}_y^{l-1}$  is the  $y^{\text{th}}$  element in the  $(l-1)^{\text{th}}$  layer,  $f_l(\cdot)$  is the activation function in the  $l^{\text{th}}$  layer,  $\mathbf{K}_{iy}^l$  represents the convolution kernel,  $*$  denotes the convolution operation,  $N$  is the number of input channels,  $\mathbf{b}_y^l$  denotes the bias with the convolution kernel.

In this study, the leaky rectified linear unit (ReLU) function shown in Eq (2) is utilized as the activation function:

$$\text{ReLU} \begin{cases} x, & x > 0 \\ 0, & x \leq 0 \end{cases} \quad (2)$$

After the convolution layer operation, the size of the feature matrices of the model will increase. In order to enhance the efficiency of the model and to prevent it from overfitting, a max pooling layer downsamples the output feature obtained from the previous convolution layer. It can be expressed as

$$D^l = \max \{ D_{i,j}^{l-1} \}, i \in [0, M], j \in [0, N] \quad (3)$$

where  $D^l$  is the output of the current pooling layer,  $D_{i,j}^{l-1}$  represents the output of the previous convolution layer, the superscripts  $i$  and  $j$  denote the rows and columns of the matrix,  $M$  and  $N$  is the number of rows and columns of the pooling filter.

To enhance model generalization and mitigate overfitting, a dropout regularization layer is typically introduced after the final pooling layer by randomly discarding some output features with a certain probability.

The fully-connected layer is generally placed at the end of the CNN architecture, functioning as a classifier that maps the features extracted by the preceding convolution and pooling layers onto the label space of the samples. Each element of the output denotes the probability that the input sample corresponds to the associated label. It can be calculated by Eq. (4):

$$F^l = f(\omega^l X^{l-1} + C^l), \quad (4)$$

where  $F^l$  is the output of fully-connected layer,  $\omega^l$  is the weighting coefficients,  $X^{l-1}$  is the features learned from the previous layers,  $C^l$  is the bias vector. The  $f(\cdot)$  represents the active function of Softmax [20].

### 2.2 Single-branch CNN model

For comparison, a single-branch CNN (SB-CNN) model is also adopted and presented in this paper. Within the CNN-based framework, the problem of structural damage identification is formulated as a classification task. The bridge is usually discretized into multiple segments, with various damage severities considered for each segment. The total number of potential damage scenarios thus corresponds to the number of classification labels required for SB-CNN model. Specifically, structural acceleration responses under different damage cases are labeled to construct training and testing dataset. These dataset are then fed into the SB-CNN model for training and subsequent damage classification. The architecture of the SB-CNN model used in this study is designed as shown in Fig. 1.

To train the weighting coefficients of the CNN model, a cross entropy error loss function is adopted, which is defined as:

$$f_{\text{loss}} = - \sum_{k=1}^N \log t_k F_k \quad (5)$$

where  $F_k$  is the output of model,  $t_k = 1$  with correct classification and  $t_k = 0$  with error classification,  $N$  is the length of output vector of FC layers.

The adaptive moment estimation (Adam) algorithm [21] is used to train the CNN model. After the optimally trained has been finished, the new structural response data under unknown damage cases can be inputted the trained CNN model for damage classifying. Therefore, the structural damage location and degree can be achieved.

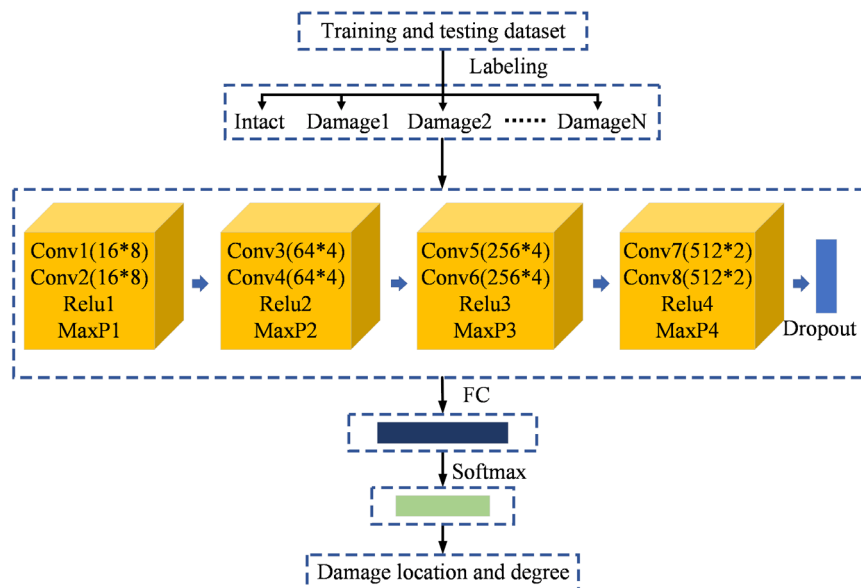


Fig. 1 Architecture of the single branch CNN model

When there is single location damage in a structure, the number of structural damage cases including the damage location and the degree of damage is small. For example, if one damage location and five damage levels are involved for a structure with 10 segments, there will be totally 51 damage cases and classification labels including intact status. However, when the structural damage occurs at multiple locations simultaneously, the damage cases will be greatly increased, resulting in a sharp increase of the classification labels. The total damage classification labels can be calculated by Eq. (6):

$$N_c = 1 + \sum_{k=1}^K (C_M^k \times D^k), \quad (6)$$

where  $K$  is the maximum number of damaged segments,  $M$  is the number of beam segments,  $D$  is the number of damage degree,  $C$  is Permutation combination operator.

For example, if the same damage occurs at two locations and five levels are considered at each damage location, there are total 276 damage classification labels. If the different damages at two locations are taken into account, the damage cases will reach 1176.

If a single branch network model is still adopted, a large number of damage cases will need a complex classification model with more learnable parameters, which will induce a heavy computation consume and even degradation of damage identification accuracy.

### 2.3 Dual-branch CNN model

To overcome the limitations of the SB-CNN model in identifying simultaneous multi-locations damage, this study

proposes an improved method using a dual branch CNN (DB-CNN) model. This architecture decomposes the identification task into two parallel sub-tasks: damage localization and damage quantification. The input data is assigned two distinct label sets, corresponding to damage location and damage severity. Every branch is trained to extract features relevant to its specific label set. Consequently, the fully-connected layer yield two independent outputs: the predicted damage location and the predicted damage degree. The final damage state of the structure is then determined by integrating the outputs from both branches. The architecture of the proposed DB-CNN model is shown in Fig. 2.

Similar to the SB-CNN model, the DB-CNN model includes eight convolution layers, four polling layers, one dropout layer. After that, the model is split into two input and output branches, which will be trained separately using damage location label dataset and damage degree label dataset. Instead of a FC layer that convert the feature maps into a one-dimensional vector in single branch CNN models, a global average pooling (GAP) layer is introduced in each branch. The GAP layer outputs a fixed-length vector by averaging each feature map output from the previous layer. Compared with the fully connected layer, the training parameters are greatly reduced, therefore, the complexity of the model is reduced and the risk of overfitting is reduced. Only the average value of each feature map is needed to feed into the softmax layer, and the calculation consumption is much less than that of the fully connected layer, which improves the efficiency of the model. It averages each feature map globally and retains global spatial information, while

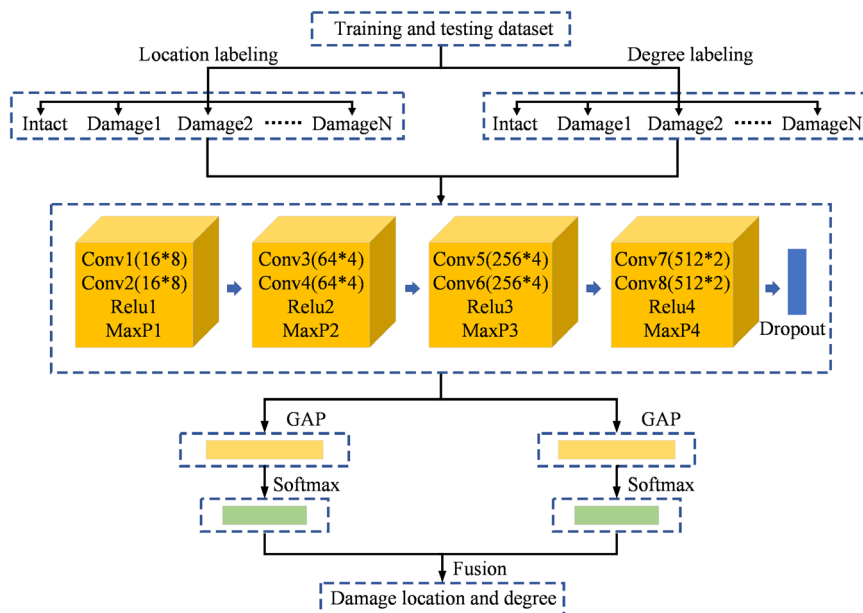


Fig. 2 Architecture of the dual branch CNN model

the fully connected layer loses this information, therefore it makes the model is more robust and adapt to the variation of input. Finally, a fusion layer is added to combine the outputs of two branches to identify structural damage location and degree.

The DB-CNN model splits the damage identification task into damage location detection and damage severity evaluation through two branches with different classification labels. Now the total classification labels can be calculated as sum of two types of labels of damage location and degree:

$$N_c = N_l + N_d = \left(1 + \sum_{k=1}^K C_M^k\right) + \left(1 + \sum_{k=1}^K D^k\right) \quad (7)$$

where  $N_l$  is the number of damage location label,  $N_d$  is the number of damage degree label.

Similar to the SB-CNN model, if the different damages at single and two locations with five levels are taken into account, the number of location labels  $N_l$  is 56, and that of the damage degree labels  $N_d$  is 31. It has greatly reduces the number of classification labels and computational complexity of the model, and it improves training and computational efficiency.

### 2.4 Multi-branch CNN model

Although the dual-branch CNN (DB-CNN) reduces the complexity compared to a single-branch model, it still requires 87 classification labels for scenarios involving single- or dual-location damage. To overcome this limitation, this study further proposes a multi-branch CNN (MB-CNN) model based on the dual-branch concept. The MB-CNN partitions the network into multiple input and output branches, corresponding to the number of structural segments. Each branch is dedicated to identifying

the damage degree of a specific segment and is trained using datasets associated with damage in that segment. Consequently, each branch independently extracts features relevant to the damage condition of its corresponding segment. The final structural damage identification is achieved by fusing the outputs from all branches. The architecture of the proposed MB-CNN model is shown in Fig. 3.

Here the total damage classification labels can be calculated as sum of labels of damage degree of all branches:

$$N_c = M \times (D + 1) \quad (8)$$

where  $M$  is the number of beam segments,  $D$  is the number of damage degree.

As mentioned in Section 2.4, if a structure containing ten segments occurs damage at a single or two locations with five levels, there are only 6 damage labels (including structural intact status) for each branch. The total number of classification labels would be 60, and it does not change with the increase of the number of damage location.

### 2.5 Model training and damage identification

Given the scarcity of real-world structural damage data, numerical analysis is employed to simulate various damage scenarios. First, a finite element model of the bridge is established. The main girder is longitudinally discretized into multiple segments, and different damage severities are simulated and analyzed for each segment. To address the low signal-to-noise ratio associated with conventional ambient excitation, a known inspection vehicle is modeled to traverse the bridge. A transient analysis is then conducted for each damage case to extract the vertical acceleration of the end nodes of each segment, thereby generating a comprehensive set of damage samples.

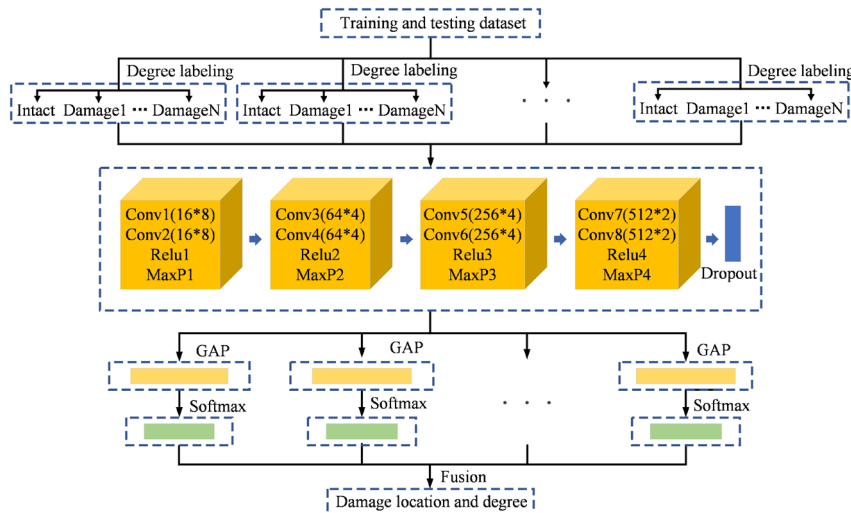


Fig. 3 Architecture of the multi-branch CNN model

The resulting dataset is partitioned into training, validation, and test sets according to a specified ratio. The training set is fed into the established CNN model for optimized training, while the validation set is used to evaluate the loss and accuracy after each epoch. By minimizing the loss function, the CNN model continuously adjusts its parameters during training, enhancing its ability to accurately predict unseen data.

Upon the completion of optimal trained, the trained CNN model can be deployed to classify new structural response data corresponding to unknown damage cases, thereby identifying both the location and severity of structural damage.

### 3 Experimental validation

#### 3.1 Experimental model

Experimental test was carried out on a simply supported T-beam model with various damage cases in the laboratory to verify the applicability of the proposed method. The T-beam model was made of acrylic board, the density and mass of the beam was  $1070 \text{ kg/m}^3$  and  $3.852 \text{ kg}$ . It consisted of a  $14 \text{ cm}$  wide flange plate and a  $5 \text{ cm}$  high web plate, and the thickness of flange and web was  $1 \text{ cm}$ . The whole length of the T-beam is  $200 \text{ cm}$ . Two holes were drilled at the centroid of the section  $2 \text{ cm}$  away from the ends of the web, and two steel bars were inserted into the holes and fixed on the two bearing, respectively. Therefore, the span of the model is  $196 \text{ cm}$ .

The beam model was divided into 10 segments, and total of 9 acceleration sensors (numbered as A1~A9) were deployed at the lower edge of the web at the end nodes

of each segments. A two-axle test vehicle was designed. The front and rear axle weights were  $0.626 \text{ kg}$  and  $0.374 \text{ kg}$ , and the wheelbase was  $10 \text{ cm}$ . A leading beam and tailing beam were installed at the both sides of the main beam to ensure that the test vehicle could pass through the model at constant speed. Two limit holes were set at the both end of the vehicle, and a steel wire was fixed above the beam model through the hole to ensure that the vehicle could pass the main beam in a straight line. A motor was installed at the end of the tail beam, which would pull the test vehicle through the main beam at constant speed. As derived in Section 2, the proposed damage identification method is based on the acceleration response of the bridge over the entire process of a vehicle entering and exiting the bridge. To accurately determine the moments when the vehicle enters and leaves the bridge, two strain sensors that were denoted as S1 and S2 were installed on leading and trailing beam at  $2 \text{ cm}$  away from the ends of the main beam. The measured stress peaks when the wheel passes the strain sensor position are used to evaluate the moment when the vehicle cross the bridge. The detail dimension of the model and the layout of measurement points were shown in Fig. 4.

For calibrating the elastic modulus of model to ensure building accurate finite element model, a static load test was carried out as follows:

- Firstly, the model was installed with simply supported form, and a mass block was placed at the mid-span of the beam as initial load.

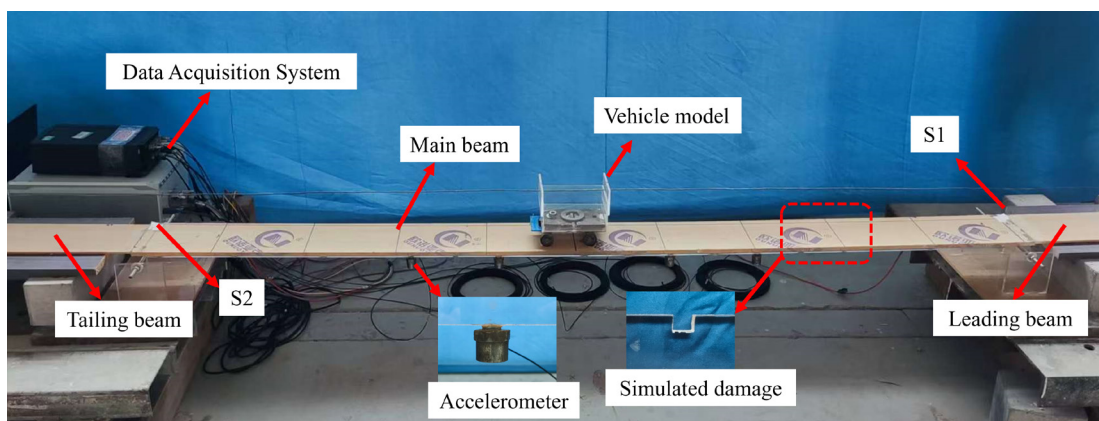
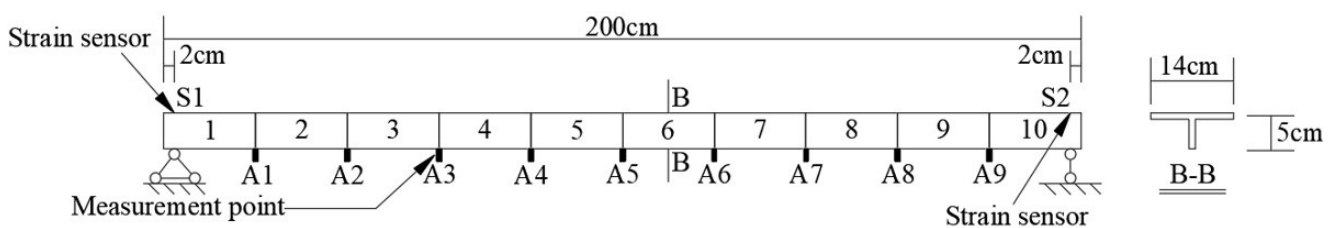


Fig. 4 The whole experimental model and the layout of measurement points

- Secondly, five mass blocks with mass of 0.224, 0.138, 0.251, 0.157, and 0.196 kg were gradually applied on the beam, each test added one mass block on the basis of the previous test, and then the structural deflection at the mid-span under each level of loading would be measured. The collected data were analyzed and fitted by the least-squares method to obtain the load-deflection relationship curve, as shown in Fig. 5.
- Finally, the elastic modulus of model could be deduced as  $E = 2.28$  GPa based on the theoretical relational between load and deflection.

It should be noted that this study mainly focuses the extracting features of structure before and after damage and damage diagnosis by the proposed method, and the absolute mechanical response of the structure is not our primary objective. Therefore, the similarity principle is not strictly considered, however this does not affect the validation results.

### 3.2 Damage tests

To validate the efficient of the proposed method for different damage cases, five same model beams were made. Firstly, a single-location damage with different damage level was simulated at different segment locations on each beam. After testing was finished, new location damage was added to every beam model for testing of multiple-location damage cases. The structural damage was simulated by cutting part of the web of a given beam segment, and the degree of damage was defined by the ratio of the sectional moment of inertia before and after damaged. Web sections with length of 1 cm and height of 0.3 cm, 0.4 cm, 0.5 cm, 0.6 cm and 1 cm were cut at the mid-span of beam segments to simulate different degrees of damage, which damage degree were 14.7%, 22.1%, 27.1%, 31.8%

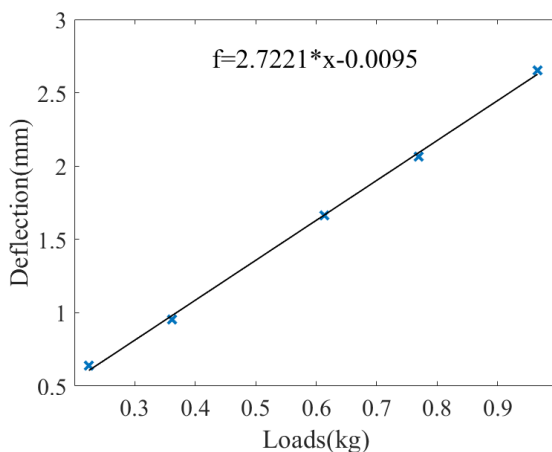


Fig. 5 Tested deflection under various level of loads

and 48.7%, respectively. The damage degree labels were divided into 5 levels as listed in Table 1.

A total of 25 damage cases including single and multi-location damage with different damage levels were simulated, the detail damage cases were listed in Table 2.

After the whole experimental model was assembled, the motor switch is turned on to pull the test vehicle through the main beam. The strain and acceleration response of the main beam would be measured with sampling frequency of 2000 Hz. Repeat the test for 3 times under each damage cases. Take Case 9 as an example, the collected stain and acceleration response of measurement point A1 was shown in Fig. 6.

Table 1 Damage degree category labels for all the damaged cases

Damage degree	Category label
Intact	L0
(0%–15%)	L1
(15%–25%)	L2
(25%–35%)	L3
(35%–45%)	L4
(45%–55%)	L5

Table 2 Damage cases of experimental test

Case	Damaged segment	Damage degree	Case	Damaged segment	Damage degree
1	None	Intact (L0)	14	D3, D6	48.7%, 48.7% (L5, L5)
2	D3	14.7% (L1)	15	D4, D5	48.7%, 48.7% (L5, L5)
3	D3	27.1% (L1)	16	D4, D7	22.1%, 22.1% (L2, L2)
4	D3	48.7% (L5)	17	D4, D7	22.1%, 31.8% (L2, L3)
5	D4	22.1% (L2)	18	D4, D7	22.1%, 48.7% (L2, L5)
6	D5	14.7% (L1)	19	D4, D7	31.8%, 48.7% (L3, L5)
7	D5	27.1% (L2)	20	D4, D7	48.7%, 48.7% (L5, L5)
8	D5	48.7% (L5)	21	D8, D5	31.8%, 22.1% (L3, L2)
9	D8	22.1% (L2)	22	D8, D5	31.8%, 31.8% (L3, L3)
10	D8	31.8% (L3)	23	D8, D5	31.8%, 48.7% (L3, L5)
11	D9	14.7% (L1)	24	D8, D5	48.7%, 48.7% (L5, L5)
12	D9	27.1% (L3)	25	D8, D9	48.7%, 48.7% (L5, L5)
13	D9	48.7% (L5)			

Note: D3 means that the third beam segment occur damage.

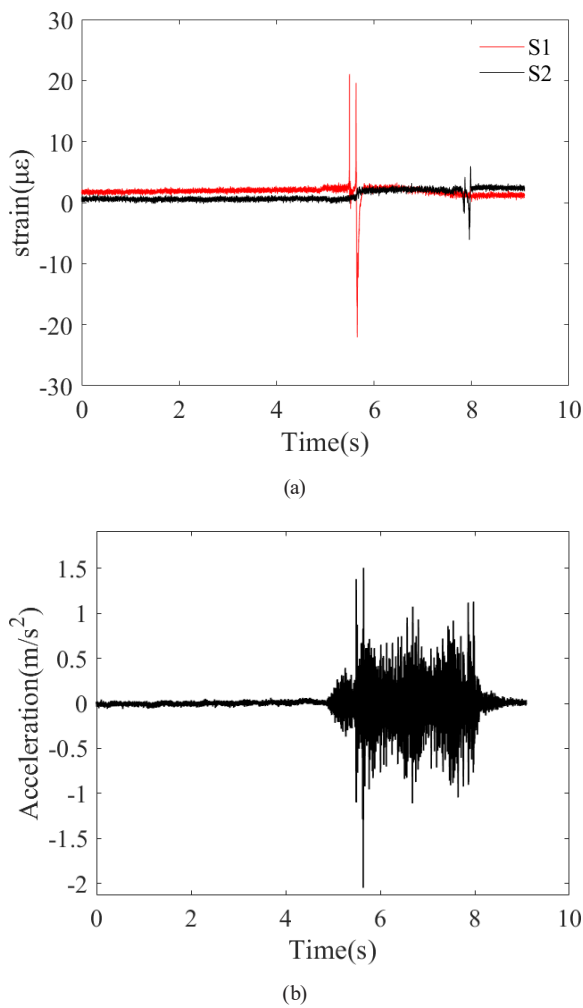


Fig. 6 Structural response under case 9 (a) strain (b) acceleration of A1

The moment when the vehicle got on and off the bearing position could be accurately determined based on the strain response data. As shown in Fig. 6 (a), when the front axle of the vehicle passed through the section of strain measurement point S1, the strain response had a peak value at  $t_1 = 5.495$  s, and the strain peak of measurement point S2 occurred at  $t_2 = 7.979$  s when the rear axle of the vehicle passed through the sensor position, so the corresponding acceleration response could be extracted.

### 3.3 Generation of damage samples

The CNN model needs a large number of samples for training, which is difficult to obtain in practical engineering. Therefore, numerical analysis will be used here to simulate various damage cases. Firstly, based on the experimental model parameters, the finite element model could be established using University Software of ANSYS [22]. As shown in Fig. 4, the beam was divided as ten segments, and each segment was discretized into 40 elements. For any beam segment, two elements in the mid-span of segment were simulated to be damaged. A total of 5 levels damage

were set for each beam segment by reducing elastic modulus from 10% to 50% at 10% intervals. For the single-position damage case, there were 50 damage cases. If the same degree of damage occurred in two beam segments simultaneously, there would be 1125 damage cases. Together with the intact condition of the structure, there were a total of 1176 types of damage cases. The two-axle testing vehicle was employed to excite the model, and transient analysis was performed under every damages case. Therefore, structural dynamic response under all cases could be obtained. The vertical acceleration response of the end points from A1 to A9 could be extracted to form damage samples, a total of 10584 groups of sample data were obtained. For enlarging the number of damage samples and considering the influence of noise, 20% (defined as the ratio of noise variance to signal variance) Gaussian white noise were added to each acquired acceleration response signals 10 times. Fig. 7 showed the simulated acceleration response of A3 and A8 when 30% damage occurred in the eighth beam segment.

All these damage sample data would be randomly divider into training set, validation set and testing set in the ratio of 6:2:2.

### 3.4 Generation of damage samples

For comparative analysis, the ingle branch, dual branch and multi-branch CNN model shown in Figs. 1–3 would be built. For SB-CNN model, including single and double damage, there were 1176 types of damage cases, all the training and validation data were labeled from 0 to 1175 according to the damage location and degree, which 0 denoted structural intact status. For the DB-CNN model, there were 56 types of damage locations and 31 damage degree including health status. Therefore, the category labels for identifying damage locations were defined from 0 to 55, the other labels for

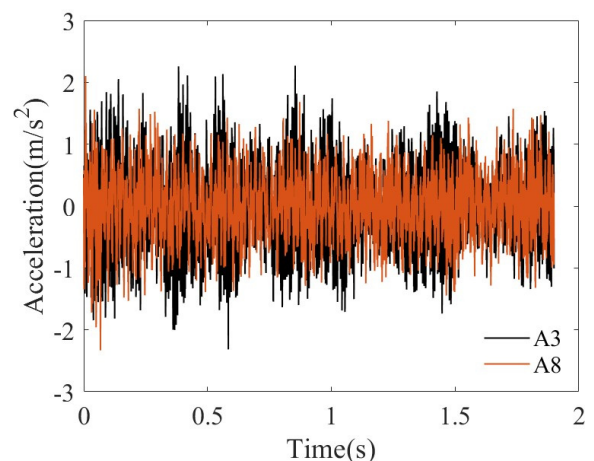


Fig. 7 Simulated acceleration response of A3 and A8

damage degree were defined from 0 to 30. However, for the MB-CNN model, each branch had six types of damage cases, and the ten branches had 60 damage cases in total. The number of classification labels of DB-CNN and MB-CNN model were much less than that of SB-CNN model.

The training and validation sets were fed into the three models for iterative training, respectively. The training was processed based on Keras2.9.0 framework. The hardware configuration was CPU Intel(R) Core(TM) i9-13900Hx, 16G of memory, GPU GeForce RTX 4060.

For comparing the identification effect when damage occur single and double position, the corresponding damage samples were fed into the SB-CNN model for trained separately. The training processes were shown in Fig. 8 (a) and (b), respectively.

Subsequently, the DB-CNN and MB-CNN models are also optimally trained. The optimized hyper-parameters for all the models and training results were listed in Table 3.

For SB-CNN model, when only a single damage occur, every epoch calculation takes 20 s, and it can effective identify damage with accuracy of 94% at validation set. When two damage occur simultaneously, every epoch calculation takes 48 s, and the identification accuracy decrease

to 82% at validation set. The increase of training consumption is mainly due to the fact that the training set is considerably larger. However, it takes 25 s and 26 s to finish epoch training for the DB-CNN and MB-CNN model, respectively. They achieve a higher computational efficiency. It can also be seen that the DB-CNN and MB-CNN model converges faster than the SB-CNN model. In additional, the identification accuracy of DB-CNN and MB-CNN model still reach to 95% and 92% at validation set, which is comparable to the identification results of the SB-CNN model under single damage case.

In additional, all damage samples data include 20% stochastic noise, it indicates that the anti-noise performance of the build models are good.

### 3.5 Damage identification

The measured data was fed into three trained CNN models for structural damage identification. When only single damage occurs, the identification results of three models are shown in Fig. 9. For the cases of damage in two positions simultaneously, the corresponding recognition results are shown in Fig. 10. And the detail identified accuracy is listed in Tables 4 and 5, respectively.

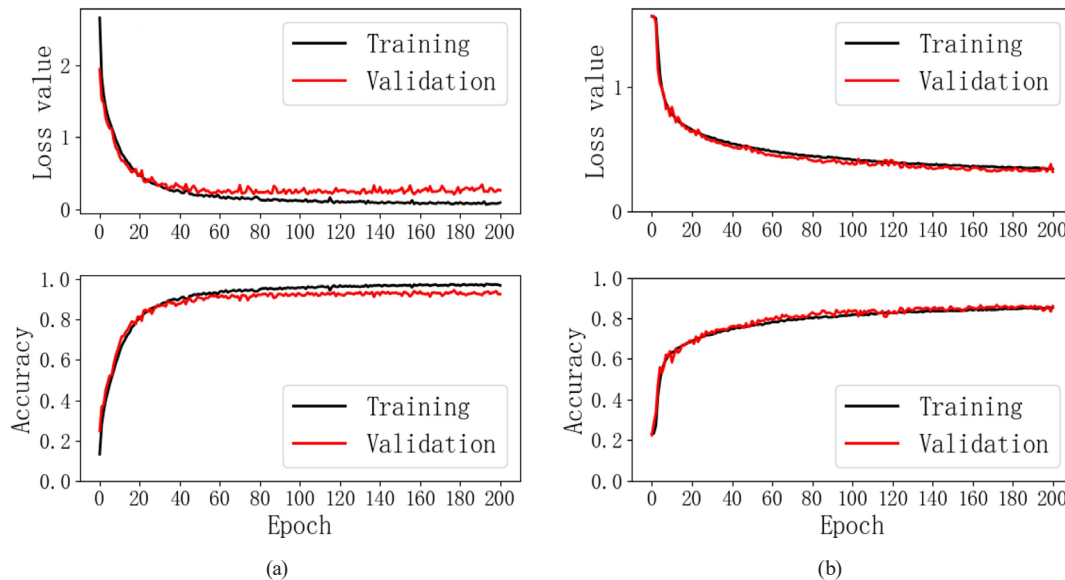


Fig. 8 Training process of SB-CNN model: (a) with single damage; (b) with double damage

Table 3 Hyper-parameters configuration and training result

Model	Batch size	Epoch	Dropout	Learning rate	Training time per epoch	Accuracy of validation set
SB-CNN (S)	256	200	0.3	0.001	20s	94%
SB-CNN (D)	256	200	0.3	0.0001	48s	82%
DB-CNN	256	200	0.3	0.001	25s	95%
MB-CNN	256	200	0.3	0.001	26s	92%

Note: SB-CNN(S) denotes only a single damage occur, SB-CNN(D) means that damage include single and two position.

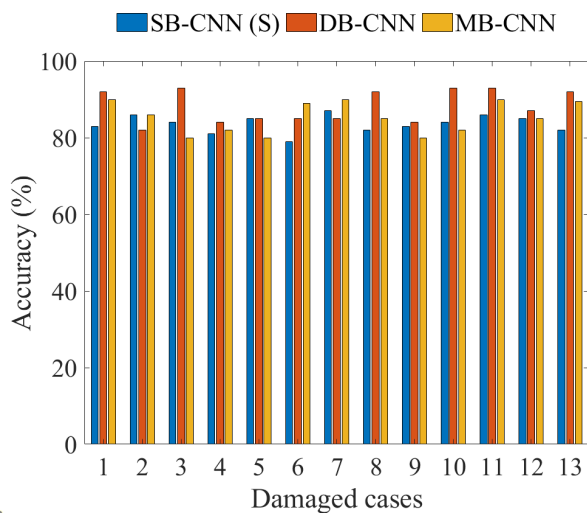


Fig. 9 Identified accuracy of three models under cases of single damage

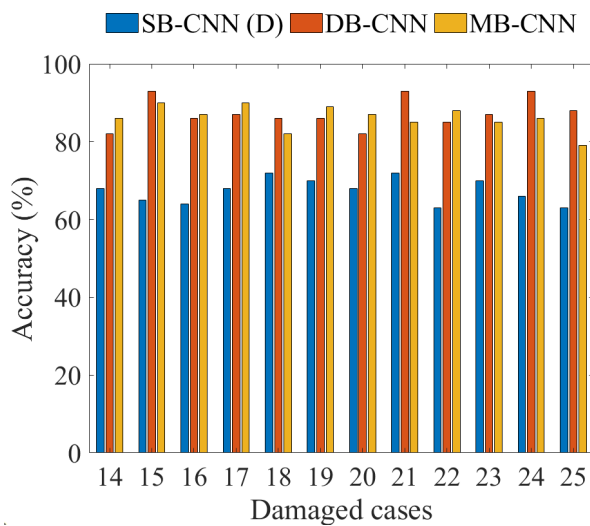


Fig. 10 Identified accuracy of three model under cases of damage in two locations

When there is only a single damage, three models can identify all of damage cases well, and the average identification accuracy is 83.6%, 88.2%, 85.3% under the 13 damage cases, respectively. When two segments are damaged, the identification accuracy of SB-CNN model decreases

Table 5 The average identification accuracy under cases of damage in two locations

Model	Damage case						Average accuracy
	14	15	16	17	18	19	
SB-CNN(D)	68%	65%	64%	68%	72%	70%	
DB-CNN	82%	93%	86%	87%	86%	86%	
MB-CNN	86%	90%	87%	90%	82%	89%	
	20	21	22	23	24	25	
SB-CNN(D)	68%	72%	63%	70%	66%	63%	67.4%
DB-CNN	82%	93%	85%	87%	93%	88%	87.3%
MB-CNN	87%	85%	88%	85%	86%	79%	86.2%

sharply to 67.4%, which mainly due to too many classification labels lead to increase of training complexity and overfitting. However, the identification accuracy of DB-CNN and MB-CNN models vary little, reaching to 87.3% and 86.2%, respectively. The Introduction of multi-branch and separation of multi-task have greatly reduced the number of classification labels, and the GAP layer decreased overfitting. Therefore, DB-CNN and MB-CNN model make better identification accuracy than SB-CNN model. It can be predicted that if more beam segments occur damage simultaneous, the number of classification labels for SB-CNN and DB-CNN model will increase dramatically, which will further reduce the identification accuracy. However, the MB-CNN model has relatively much less increase in classification labels, and it has more advantage in identifying multiple damages.

To investigate the influence of different measurement points on damage diagnosis, the simulated damage samples at each measurement points (A1~A9) were extracted separately, and then they were fed into the trained model to diagnosis structural damage. So the average identification accuracy of each measurement points is calculated individually based on the diagnosis results of the corresponding measurement point. And the detailed identified results are shown in Fig. 11 and Table 6.

Table 4 The identification accuracy under cases of single damage

Model	Damage case							Average accuracy
	1	2	3	4	5	6	7	
SB-CNN(S)	83%	86%	84%	81%	85%	79%	87%	
DB-CNN	92%	82%	93%	84%	85%	85%	85%	
MB-CNN	90%	86%	80%	82%	80%	89%	90%	
	8	9	10	11	12	13		
SB-CNN(S)	82%	83%	84%	86%	85%	82%		83.6%
DB-CNN	92%	84%	93%	93%	87%	92%		88.2%
MB-CNN	85%	80%	82%	90%	85%	90%		85.3%

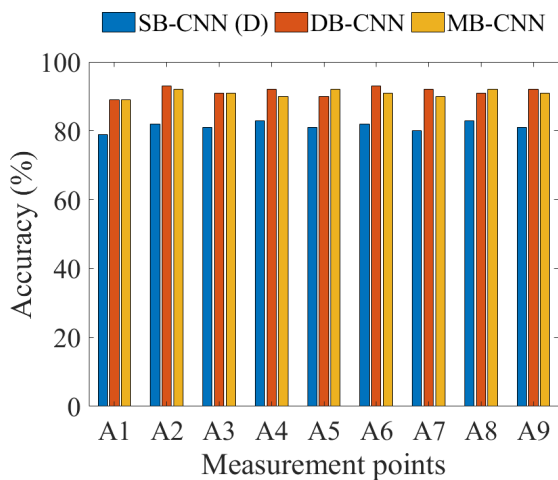


Fig. 11 The identified accuracy of each measurement point

Table 6 The average identification accuracy of each measurement point

Model	A1	A2	A3	A4	A5
SB-CNN(S)	82%	84%	83%	86%	85%
SB-CNN(D)	66%	68%	68%	70%	69%
DB-CNN	86%	88%	89%	89%	87%
MB-CNN	85%	88%	84%	87%	83%
	A6	A7	A8	A9	
SB-CNN(S)	84%	82%	85%	83%	
SB-CNN(D)	67%	68%	69%	70%	
DB-CNN	86%	89%	87%	88%	
MB-CNN	86%	86%	85%	88%	

It can be seen that for each model, the identification accuracy of all the measuring points has little difference. Therefore, the effect of damage identification is insensitive to the distance between sensor and damage location. It mainly because the moving vehicle load must pass through the structural damage location, which will better provoke the structural damage characteristics. It means that it is possible to achieve structural damage identification without densely deploying sensors, which is convenient for practical engineering application.

#### 4 Conclusions

In this study, a damage identification method based on dual-branch and multi-branch CNN models under moving loads is developed. The performance of the two proposed models is validated and compared with that of a conventional single-branch CNN model through an experimental test on a simply supported beam subjected to a moving vehicle. Based on the analysis results, the following conclusions can be drawn:

1. The DB-CNN and MB-CNN models train more efficiently and converge faster than the SB-CNN model. Additionally, the proposed method exhibits stronger noise robustness.

2. Experimental results further confirm the accuracy and effectiveness of the proposed approach. Under 13 single-damage scenarios, the average identification accuracy of the SB-CNN, DB-CNN, and MB-CNN models is 83.6%, 88.2%, and 85.3%, respectively. For 12 double-damage scenarios, the corresponding accuracy rates are 67.4%, 87.3%, and 86.2%. The performance of the SB-CNN model degrades significantly under multiple-damage conditions, whereas the DB-CNN and MB-CNN models show only minor variations in performance. This can be attributed to the reduced classification labels, which lower training complexity, and the incorporation of a Global Average Pooling (GAP) layer, which mitigates overfitting. It can be anticipated that a further increase in the number of damage categories would continue to impair the accuracy of the SB-CNN and DB-CNN models. Thus, the MB-CNN model demonstrates greater advantages in multi-damage identification.
3. The damage identification results show no obvious variation across sensors placed at different positions for the same damage case. This is primarily because moving vehicle loads excite structural damage features more effectively than ambient vibrations when passing over damaged regions. Consequently, it is feasible to identify structural damage without densely distributed sensors, which enhances the practicality of the method for real-world engineering applications.

The proposed method in this paper is based on a simply supported beam bridge. When it is applied to more complex structure, some challenges issues require further in-depth investigation:

1. It relies on supervised learning, leading to limited applicability to damage scenarios unseen during model training.
2. Various damage samples are often difficult to obtain in practice, how to accurately simulate various practical structural damage cases is a great challenge by numerical model. Maybe transfer learning technique is a potential solution to these problems.

#### Acknowledgement

This research is financially supported by the National Natural Science Foundation of China (Grant No. 52378290). The authors would also like to thank the reviewers for their suggestions which permit to improve this manuscript.

## References

- [1] Bakhshizadeh, A., Sadeghi, K., Ahmadi, S., Royaei, J. "Damage Identification in Long-Span Cable-Stayed Bridges Under Multiple Support Excitations", *International Journal of Civil Engineering*, 21(8), pp. 1275–1290, 2023.  
<https://doi.org/10.1007/S40999-023-00823-7>
- [2] Wang, C. "Overview of integrated health monitoring system installed on cable-stayed bridge and preliminary analysis of results", *Gradevinar*, 73(6), pp. 591–604, 2021.  
<https://doi.org/10.14256/JCE.2940.2020>
- [3] He, W-Y., He, J., Ren, W-X. "Damage localization of beam structures using mode shape extracted from moving vehicle response", *Measurement*, 121, pp. 276–285, 2018.  
<https://doi.org/10.1016/j.measurement.2018.02.066>
- [4] Yan, W-J., Ren, W-X., Huang, T-L. "Statistic structural damage detection based on the closed-form of element modal strain energy sensitivity", *Mechanical Systems and Signal Processing*, 28, pp. 183–194, 2012.  
<https://doi.org/10.1016/j.ymsp.2011.04.011>
- [5] Shahsavari, V., Chouinard, L., Bastien, J. "Wavelet-based analysis of mode shapes for statistical detection and localization of damage in beams using likelihood ratio test", *Engineering Structural*, 132, pp. 494–507, 2017.  
<https://doi.org/10.1016/j.engstruct.2016.11.056>
- [6] Bao, C., Hao, H., Li, Z-X. "Multi-stage identification scheme for detecting damage in structures under ambient excitations", *Smart Materials and Structures*, 22(4), 045006, 2013.  
<https://doi.org/10.1088/0964-1726/22/4/045006>
- [7] Dong, Y., Li, Y., Lai, M. "Structural damage detection using empirical-mode decomposition and vector autoregressive moving average model", *Soil Dynamics and Earthquake Engineering*, 30(3), pp. 133–145, 2010.  
<https://doi.org/10.1016/j.soildyn.2009.10.002>
- [8] Kong, X., Cai, C. S., Kong, B. "Damage Detection Based on Transmissibility of a Vehicle and Bridge Coupled System", *Journal of Engineering Mechanics*, 141(1), 04014102, 2014.  
[https://doi.org/10.1061/\(ASCE\)EM.1943-7889.0000821](https://doi.org/10.1061/(ASCE)EM.1943-7889.0000821)
- [9] Nie, Z., Guo, E., Li, J., Hao, H., Ma, H., Jiang, H. "Bridge condition monitoring using fixed moving principal component analysis", *Structural Control and Health Monitoring*, 27(6), e2535, 2020.  
<https://doi.org/10.1002/stc.2535>
- [10] Chen, Z-W., Zhu, S., Xu, Y-L., Li, Q., Cai, Q-L. "Damage Detection in Long Suspension Bridges Using Stress Influence Lines", *Journal of Bridge Engineering*, 20(3), 05014013, 2014.  
[https://doi.org/10.1061/\(ASCE\)BE.1943-5592.0000681](https://doi.org/10.1061/(ASCE)BE.1943-5592.0000681)
- [11] Zheng, X., Yang, D-H., Yi, T-H., Li, H-N. "Bridge influence line identification from structural dynamic responses induced by a high-speed vehicle", *Structural Control and Health Monitoring*, 27(7), e2544, 2020.  
<https://doi.org/10.1002/stc.2544>
- [12] Wang, C., Pan, X., Qi, T-Y., Han, G-N., Ren, W-X. "Damage Identification of Simple Supported Bridges Under Moving Loads Based on Variational Mode Decomposition and Deep Learning", *International Journal of Structural Stability and Dynamics*, 25(6), 25500065, 2025.  
<https://doi.org/10.1142/S0219455425500658>
- [13] Abdeljaber, O., Avci, O., Kiranyaz, S., Gabbouj, M., Inman, D. J. "Real-time vibration-based structural damage detection using one-dimensional convolutional neural networks", *Journal of Sound and Vibration*, 388, pp. 154–170, 2017.  
<https://doi.org/10.1016/j.jsv.2016.10.043>
- [14] Lin, Y.Z., Nie, Z.H., Ma, H.W. "Structural Damage Detection with Automatic Feature-Extraction through Deep Learning", *Computer-Aided Civil and Infrastructure Engineering*, 32(12), pp. 1025–1046, 2017.  
<https://doi.org/10.1111/mice.12313>
- [15] Yu, Y., Wang, C., Gu, X., Li, J. "A novel deep learning-based method for damage identification of smart building structures", *Structural Health Monitoring*, 18(1), pp. 143–163, 2019.  
<https://doi.org/10.1177/1475921718804132>
- [16] Azimi, M., Pekcan, G. "Structural health monitoring using extremely compressed data through deep learning", *Computer-Aided Civil and Infrastructure Engineering*, 35(6), pp. 597–614, 2020.  
<https://doi.org/10.1111/mice.12517>
- [17] Li, D., Liang, Z-L., Ren, W-X., Yang, D., Wang, S-D., Xiang, S-L. "Structural damage identification under nonstationary excitations through recurrence plot and multi-label convolutional neural network", *Measurement*, 186, 110101, 2021.  
<https://doi.org/10.1016/J.MEASUREMENT.2021.110101>
- [18] Zhang, Y., Miyamori, Y., Mikami, S., Saito, T. "Vibration-based structural state identification by a 1-dimensional convolutional neural network", *Computer-Aided Civil and Infrastructure Engineering*, 34(9), pp. 822–839, 2019.  
<https://doi.org/10.1111/mice.12447>
- [19] Xue, Z., Xu, C., Wen, D. "Structural Damage Detection Based on One-Dimensional Convolutional Neural Network", *Applied Sciences*, 13(1), 140, 2023.  
<https://doi.org/10.3390/AP13010140>
- [20] Zhan, Y., Lu, S., Xiang, T., Wei, T. "Application of convolutional neural network in random structural damage identification", *Structures*, 29, pp. 570–576, 2021.  
<https://doi.org/10.1016/j.istruc.2020.11.056>
- [21] Kingma, D. P., Ba, J. "Adam: A Method for Stochastic Optimization", presented at ICLR 2015, San Diego, CA, USA, May, 7–9, 2015.  
<https://doi.org/10.48550/arXiv.1412.6980>
- [22] ANSYS Inc "Ansys academic research mechanical, Release 18.1", [computer program] Available at: <https://www.ansys.com/news-center/press-releases/05-16-17-ansys-18-1-expands-pervasive-engineering-simulation> [Accessed: 20 January 2026]